

Characterization and implementation of the L-alanine detector for quality control of lung SBRT treatments with the VMAT technique

Sarah J. Mazaro^a, Angela Kinoshita^{b,*}, Patricia Nicolucci^c, Leonardo Peres da Silva^a, Oswaldo Baffa^c

^a Instituto Nacional de Câncer, Rio de Janeiro, Brazil

^b UNOESTE - Universidade do Oeste Paulista, Presidente Prudente, Brazil

^c Departamento de Física – Faculdade de Filosofia, Ciências e Letras de Ribeirão Preto, Universidade de São Paulo, Ribeirão Preto, Brazil

ARTICLE INFO

Keywords:

Quality control
Alanine
Dosimetry
SBRT
VMAT

ABSTRACT

New treatments in radiotherapy have some difficulties, among them, the geometric and dosimetric characterization of the radiation beam and the use of small radiation fields. Determination of the prescribed dose in the target volume in cases of small fields is difficult due to the absence of lateral electronic equilibrium and the sharp dose gradient at the edges of the fields. In this way, the choice of the radiation detector becomes relevant when performing the dosimetry of small fields. Alanine dosimeters have proven to be a good option for measurements of high radiation doses in these field sizes. This work aims to characterize the alanine detector through dosimetric tests for the VMAT (Volumetric Modulated Arc Therapy) technique in cases of SBRT (Stereotactic Body Radiation Therapy) to demonstrate the feasibility of using the alanine dosimetric system for use in quality control. End-to-End test was performed in a phantom, simulating two situations: homogeneous and heterogeneous regions. The response of L-alanine showed a strong linear correlation with dose ($R^2 = 0.99997$), and insignificant dependence to dose rate. In the End-to-End test for a planned dose of 18 Gy, the doses obtained in alanine presented expanded uncertainty of 4.60% at 95% confidence level. Therefore, this work demonstrated that alanine dosimeter is suitable for quality control of SBRT with the VMAT technique in routine applications.

1. Introduction

Development of new equipment and more complex techniques of irradiation has turned radiotherapy more sophisticated and accurate. Among the most recent technological advances we can mention: Intensity modulated Radiation Therapy (IMRT), Volumetric Modulated Arc Therapy (VMAT), Intracranial Stereotactic Radiosurgery (SRS); Stereotactic Body Radiation Therapy (SBRT), Image Guided Radiotherapy (IGRT) (Meyer, 2011). With these technological developments, new modalities of fractionation of dose, known as hypofractionation, allow to perform the treatment in a shorter period, besides obtaining a greater localized control of the disease. The hypofractionation consists of a smaller number of sessions of higher doses, typically 1 to 5 fractions. Thus, the requirements for dose delivery are even stricter than with the

traditional treatments (Meyer, 2011).

SBRT can be defined by the precise delivery of high doses of radiation with few fractions in an extracranial target (Rubio et al., 2013). Therefore, an attractive and fast dose delivery option in these cases is using VMAT, which allows rotating the gantry with the radiation beam continuously on and modulated by the movement of the multileaf collimator (MLC). In addition, during rotation, some parameters may change simultaneously, such as gantry rotation speed and dose rate. The geometric and dosimetric characterization of these technologies, as with the VMAT, becomes complex, because it involves the use of small field segments, angular and dose rate dependencies, in addition to modulation of beam fluence that can affect the dose detector output.

As the human body has a variety of tissues and cavities with different physical and radiological properties, the irradiated volume has

Abbreviations: ESR, Electron Spin Resonance; IMRT, Intensity modulated Radiation Therapy; SBRT, Stereotactic Body Radiation Therapy; VMAT, Volumetric Modulated Arc Therapy; TLD, Thermoluminescent dosimeter; OSL, Optically Stimulated Luminescence; IC, Ionization Chamber; PTV, Planned target volume; MU, Monitor Unit.

Peer review under responsibility of The Egyptian Society of Radiation Sciences and Applications.

* Corresponding author.

E-mail addresses: angelamitie@gmail.com, angela@unoeste.br (A. Kinoshita).

<https://doi.org/10.1016/j.jrras.2022.01.002>

Received 18 June 2021; Received in revised form 28 November 2021; Accepted 13 January 2022

Available online 3 March 2022

1687-8507/© 2022 The Egyptian Society of Radiation Sciences and Applications. Production and hosting by Elsevier B.V. This is an open access article under the CC BY-NC-ND license (<http://creativecommons.org/licenses/by-nc-nd/4.0/>).

heterogeneities (Papanikolaou et al., 2004). Therefore, the determination of delivered dose in the target volume in cases as the lung, can undergo significant changes compared to that obtained for a homogeneous medium (Papanikolaou et al., 2004; Merrow et al., 2013). So, the choice of the appropriate radiation detector for such situations becomes relevant. In clinical practice, ionization chambers, diodes, radiochromic films and solid-state dosimeters (thermoluminescent dosimeters (TLD) and optically stimulated luminescent dosimeters (OSL), for example) are used. Ionization chambers are usually the standard detectors in Radiation Therapy given their response linearity with dose and low energy and dose rate dependence; diodes present high sensitivity and spatial resolution, but also high energy and dose rate dependence; radiochromic films allow the evaluation of dose distributions in 2D, but require later scanning and processing; TLDs and OSL dosimeters can show high sensitivity and spatial resolution, but have the disadvantage of requiring a late reading (Parwaie et al., 2018).

Several studies have investigated the dosimetric features of alanine/electron spin resonance (ESR) dosimeters, showing that they present high sensitivity and spatial resolution, as well as low energy and dose rate dependence (Rouihem et al., 2022; Ramírez et al., 2012; Anton et al., 2013; Anton et al., 2008). Also, studies show that L-alanine presents chemical and physical properties adequate to be used as a radiation detector in Radiation Therapy (Secerov et al., 2016; Chen et al., 2008; Abrego et al., 2007; Regulla & Deffner, 1982). The International Atomic Energy Agency (IAEA), recommend L-alanine as a radiation detector for dosimetry with high dose rate beams and for intercomparison between detectors (Sharpe et al., 1996; Onori et al., 2006). Recent studies with this detector have shown an improvement in sensitivity and expanded the possibilities of clinical applications to the new modalities of radiotherapy (Vega Ramirez et al., 2011; Baffa & Kinoshita, 2014; Rech et al., 2014; Knudtsen et al., 2016). Furthermore, for performing complex techniques, such as SBRT, it is indispensable to verify all steps to dose delivery, what is known as an End-to-End test (O'Daniel et al., 2012; Seravalli et al., 2015). This work aims to characterize the response of L-alanine detectors to irradiation and perform a feasibility study for their use in quality control of SBRT treatments with the VMAT technique, as a feasibility study.

2. Materials and methods

2.1. Alanine dosimeter

L-alanine dosimeters used in this study were produced in our group at the University of São Paulo (DF-FFLCRP-USP). A homogeneous mixture of: 90% L-alanine (Sigma Aldrich) in powder form and 10% of a binding agent, high purity paraffin ground in small particles, was pressed at 4 ton in a hardened stainless-steel casting mold. The dosimetric pellets obtained in this process have a cylindrical shape with nominal dimensions of 4 mm in diameter and 10 mm in height, mass approximately 150 mg and a density of 1.19 g/cm^3 (Baffa & Kinoshita, 2014; Ramirez et al., 2012). The alanine dosimeters don't require any pre-irradiation or pre-reading processing, such as TLDs for example. Reading is performed in an Electron Spin Resonance spectrometer, allowing reuse of the dosimeters after reading. The signal obtained is related to the integrated dose over the whole dosimeter. Usually, batches of 500 dosimeters are produced in a single preparation. The homogeneity of the response to irradiation was tested and the maximum variation found was 3%.

2.2. Phantom

The phantom used in the irradiations is composed of 17 circular acrylic (polymethyl methacrylate-PMMA) plates with a thickness of 1 cm each, 15 cm in diameter, density (ρ) of 1.18 g/cm^3 and effective atomic number $Z_{\text{eff}} = 6.81$ (Fig. 1). The plates are tighten together using four plastic screws at their edges. The alanine was positioned on the

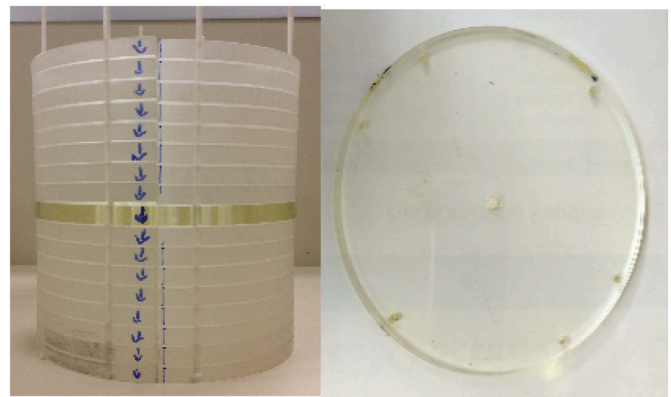


Fig. 1. Acrylic phantom used in the irradiations. a) Side view b) Axial view of the centerpiece with alanine detector positioned at the center. Each acrylic slab is 1 cm thick and the diameter is 15 cm. The arrows are used to align the slabs during assembling of the phantom.

central axis of the plaque located in the middle of the phantom.

2.3. Irradiation

Alanine dosimeters and a cylindrical ionization chamber (Pinpoint - PTW-Freiburg 31014 with 0.015 cc) connected to a PTW/UNIDOS electrometer were irradiated in a Varian Trilogy – 6 MV Linac.

The setup used for irradiation were: SSD = 100 cm, $10 \times 10 \text{ cm}^2$ field and depths of 5.5 cm for alanine and 5.75 cm for ionization chamber, as shown in Fig. 2. The small difference in positioning of the two detectors was given by the difference in thickness of the central slabs that accommodate each detector and was taken into account in the dose value calculations. The ionization chamber used is routinely inter-compared with another ionization chamber used in the clinic, calibrated and traced to a secondary standard laboratory (SSL) at the national metrological authority.

2.4. Alanine Calibration Curve

For the calibration curve, a set of Alanine dosimeters was irradiated with known doses, in a range from 1 to 35 Gy, using a dose rate of 400 MU/min and the 6 MV beam. This dose range was used because it represents the therapeutic dose range usually employed in SBRT procedures and fits the application range of the alanine dosimeter. Doses lower than 1 Gy were not employed because it is known that is difficult to obtain the required accuracy in alanine dosimeters in this dose range. The dose rate for calibrations was chosen to match the standard one for dosimetric purposes at the clinic.

The spectra of irradiated dosimeters were registered in the JEOL FA200 – X Band Electron Spin Resonance spectrometer at the Department of Physics, University of São Paulo (DF-FFLCRP-USP). The first harmonic signal was used and the peak-to-peak amplitude of the central line of the ESR spectrum was obtained for each dose (Fig. 3). The calibration curve was constructed associating the amplitude value, normalized by the dosimeter mass, with the dose.

2.5. Dependence with the dose rate

The VMAT technique varies the dose rate during irradiation and, therefore, it is necessary to evaluate the response of the L-alanine detector to irradiations with different dose rates. The Alanine dosimeters and the Ionization Chamber were irradiated with 500 MU at dose rates of 200, 300, 400, 500 and 600 MU/min. Two dosimeters were used for each dose rate measurement. The dose obtained through the Alanine Calibration Curve at an irradiation rate of 400 MU/min was used as reference, since that dose rate is used for reference dosimetric purposes

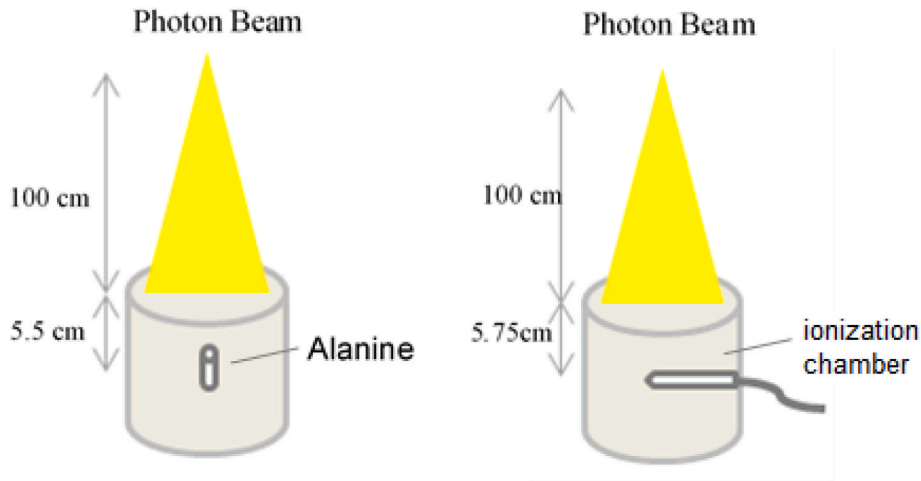


Fig. 2. Experimental setup for calibration of Alanine dosimeters and the comparison with the measurements performed with the ionization chamber.

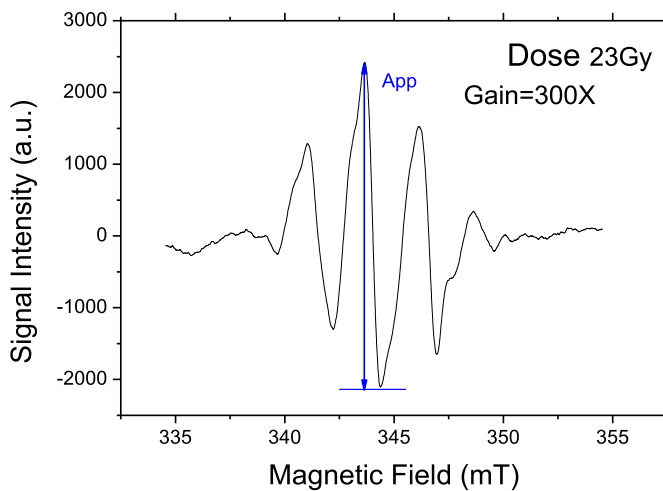


Fig. 3. ESR spectrum of L-Alanine irradiated with a dose of 23 Gy on the linear accelerator Trilogy. The peak-to-peak amplitude (A_{pp}) of the centerline, normalized by dosimeter mass was used for the calibration curve.

at the clinic and was used in the calibration irradiation of the dosimeters. To determine the correction factor of response of alanine to dose rate, the average of all doses obtained for each dose rate was normalized to the reference, according to equation (1):

$$F_{DR} = \left(\frac{D_{DR\ 400}}{D_{DRi}} \right) \quad (1)$$

where:

- F_{DR} = dose rate correction factor;
- D_{DRi} = mean dose detected for a given dose rate;
- $D_{DR\ 400}$ = dose value detected at the dose rate of 400MU/min (reference).

In addition, the dose obtained by the Alanine dosimeter was compared with that obtained by the ionization chamber for each dose rate.

2.6. Field size dependency

The dependence of the L-alanine detector with the field size was evaluated considering 5 different field sizes: $1 \times 1\text{ cm}^2$, $2 \times 2\text{ cm}^2$, 3×3

cm^2 , $5 \times 5\text{ cm}^2$ and $10 \times 10\text{ cm}^2$; fields lower than $3 \times 3\text{ cm}^2$ are considered small (Das et al., 2007). Alanine dosimeters and Ionization Chamber were irradiated with the same dose, using 500 MU, and with a dose rate of 400 MU/min as describe previously. Measurements were performed in triplicate and the average and standard deviation (SD) is reported. For comparison, the ionization chamber was used to determine the dose at each field size.

2.7. End-to-end testing

To perform the End-to-End test, the phantom of Fig. 1 was used, and also was adapted to simulate a heterogeneous medium. The phantom of homogeneous medium is composed of 17 acrylic plates (15 cm diameter and 1 cm thickness), which simulates the soft tissue. The heterogeneous phantom had its central plate replaced by another, composed of acrylic and cork, which simulates the lung (Fuse et al., 2018; Simon et al., 2006; Vanbree et al., 2014), as shown in Fig. 4. The cork disc is centered on the acrylic disc and is 6.25 cm in diameter. The alanine dosimeter was positioned in the center of both phantoms. Both phantoms were scanned in the CT x ray scanner Philips Brilliance CT Big Bore. This scanner is routinely used for acquiring the images for the treatment planning.

With the phantom’s CT images uploaded into the treatment planning system (TPS), the following structures were contoured: Detector (alanine dosimeter), PTV (planned target volume) with 1.5 cm margin of alanine and lung (cork material), as shown in Fig. 5. The 1.5 cm margin adopted in PTV was chosen because it meets the requirements that establish margin values greater than 1 cm, due to the geometric variations of the tumor (Li et al., 2016).

The dose prescription of SBRT was 18 Gy and a planning using a modulated arc lung (VMAT) with heterogeneity correction was generated, using a 6 MV beam. The dose distribution was calculated using the Eclipse TPS, Version 8.6, using the AAA (Anisotropic Analytical Algorithm) algorithm (Sterpin et al., 2007).

After the planning, the phantoms were irradiated accordingly (at the Varian Trilogy 6 MV LINAC). The spectra of the alanine dosimeters were recorded, and the dose obtained by the calibration curve was adjusted using the correction factor, according to equation (2).

$$D_{\text{Alanine}} = \text{Dose}_{\text{calibration curve}} \times F_{DR} \quad (2)$$

where:

- D_{Alanine} = Absorbed dose corrected for alanine (cGy);
- $\text{Dose}_{\text{calibration curve}}$ dose obtained through ESR signal intensity, F_{DR} dose rate correction factor.

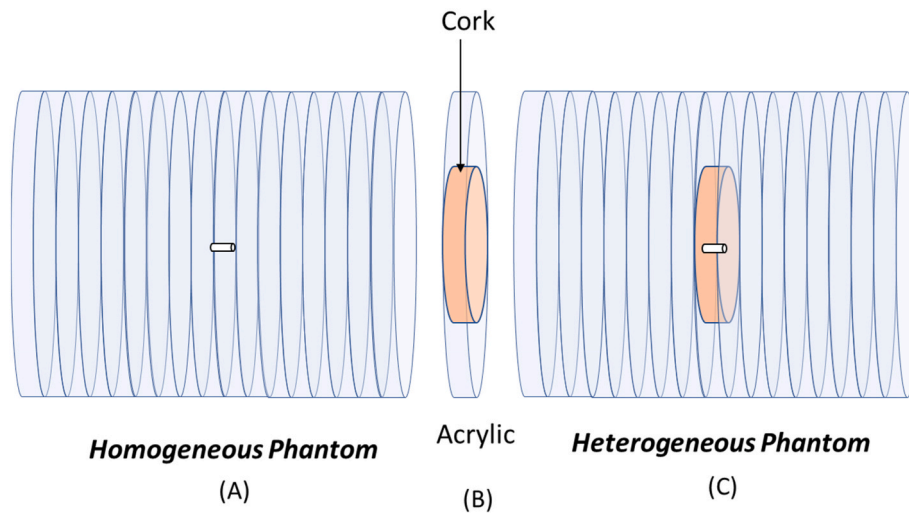


Fig. 4. Cylindrical phantoms with centralized alanine detector. a) Homogeneous (Acrylic); b) Acrylic plate with cork c) Heterogeneous (Acrylic + Cork).

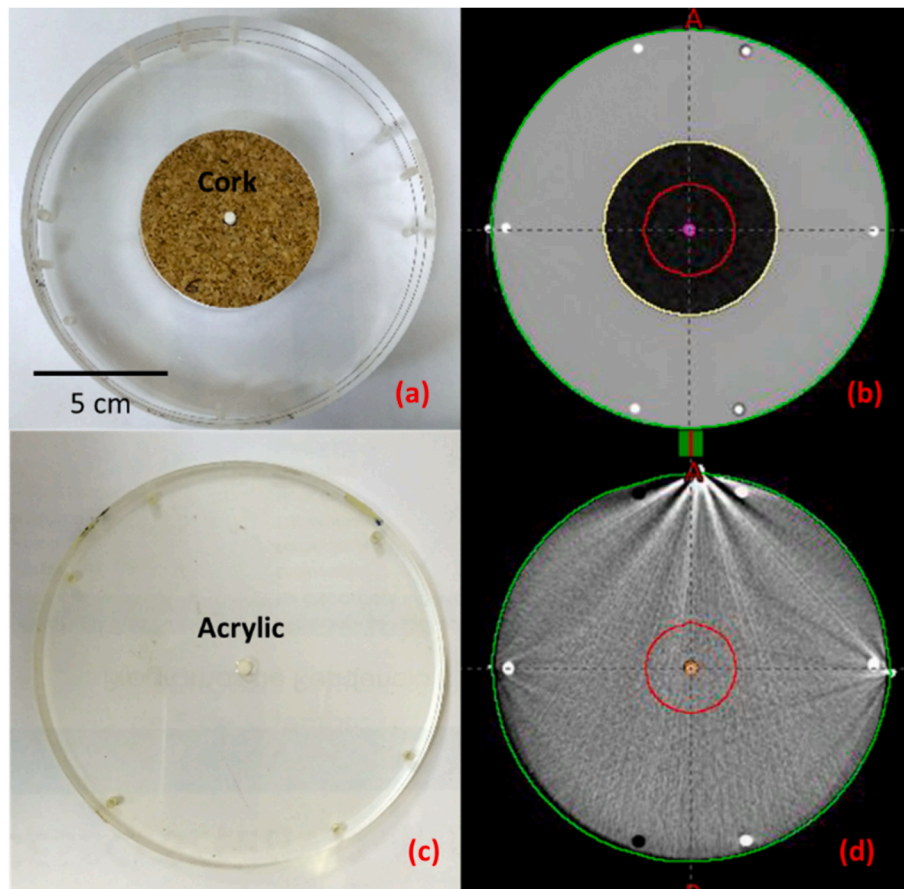


Fig. 5. Photographs of central region of the phantoms: (a) Heterogeneous phantom and (c) Homogeneous phantom. CT Images and outline of the structures (b) Heterogeneous phantom and (d) Homogeneous phantom. The red line indicates PTV (target volume), yellow line the lung and green line the phantom’s body. (For interpretation of the references to color in this figure legend, the reader is referred to the Web version of this article.)

The results were compared with the values generated by the TPS.

2008), at 95% confidence level.

2.8. Uncertainties considerations

The uncertainties were determined according to the “Guide to Expression of Measurement Uncertainty (GUM)”, given by the International Organization for Standardization (ISO/IEC GUIDE 98–3:2008,

3. Results and discussion

3.1. Calibration

The calibration curve of L-alanine is shown in Fig. 6. Linear fitting of

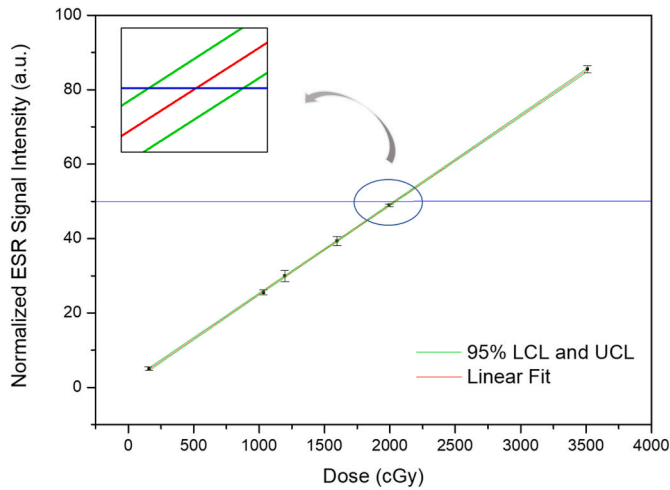


Fig. 6. Calibration curve for L-Alanine dosimeters. The vertical axis shows the ratio of the ESR signal amplitude (App) by dosimeter mass (mg). Pearson’s $r^2 = 0.99997$. Red line is the linear fitting of data, green lines are the 95% Lower and Upper Control Limits (LCL and UCL). (For interpretation of the references to color in this figure legend, the reader is referred to the Web version of this article.)

experimental data points was performed. Each point represents the average and standard deviation measurements performed in duplicate.

The amplitude of the signal resulting from alanine presented a linear response with the dose, since the correlation coefficient resulting from the linear adjustment is 0.99997. This value demonstrates the stability of the dosimeters reading and corroborates with results from literature (Alves et al., 2015; Helt-Hansen et al., 2009; Baffa & Kinoshita, 2014; Kuntz et al., 1996). The equation that relates the amplitude of the ESR spectrum and the dose was obtained using a linear fit to the experimental data and is:

$$Alanina_{(APP/Massa)} = 0.024 \text{ Dose}_{(cGy)} + 1.0095 \quad (3)$$

The uncertainty of dose associated with the calibration curve is 0.5%, considering the variation of doses between UCL and LCL as demonstrated in the inset of Fig. 5.

3.2. Dependence with the dose rate

Table 1 shows the results of the dose obtained in alanine dosimeters and in the ionization chamber for each dose rate. The dose in alanine was calculate using the calibration curve (Fig. 5) based on the ESR signal amplitude and mass. The value in the table corresponds to the average of 2 dosimeters for each dose rate. The dose in the ionization chamber was corrected according to their position in the phantom, since the alanine was at 5.5 cm depth and Ionization chamber, 5.75 cm.

The correction factor of the response of alanine to the dose rate according to equation (1) is:

$$F_{DR} = 1.00 \pm 0.05$$

Table 1
Dose in the alanine dosimeter and ionization chamber according to the dose rate.

| Dose rate (MU/min) | Alanine (cGy) | Ionization Chamber (cGy) | Dose IC/Dose alanine |
|-----------------------|------------------|-----------------------------|----------------------|
| 200 | 406 ± 12 | 400 | 0.99 |
| 300 | 405 ± 9 | 399 | 0.99 |
| 400 | 403 ± 12 | 398 | 0.99 |
| 500 | 398 ± 12 | 395 | 0.99 |
| 600 | 400 ± 11 | 397 | 0.99 |
| Mean ± SD | 402 ± 12 | 398 ± 2 | 0.99 |

The F_{DR} shows equivalence of doses obtained among different dose rates, showing that the different dose rates does not affect the doses assessed with Alanine in the dose range studied.

3.3. Dependency with field size

The dose dependence with the radiation field size for both the alanine and the ionization chamber (IC) are shown in Fig. 7. As expected, for irradiation fields smaller than $10 \times 10 \text{ cm}^2$ there is a decrease in the deposited dose.

In general, alanine had a greater response than that obtained by ionization chamber and this agrees with Alfonso et al. (Alfonso et al., 2008), which demonstrates that alanine has a better electronic equilibrium condition. The largest difference (13.5%) was found for the $1 \times 1 \text{ cm}^2$ field size. This difference may become significant in cases of high doses in the lung, where there are regions of heterogeneities and the planning system needs to be proper data feed (Vega et al., 2014). Usually, the average size of the lesion is larger than $1 \times 1 \text{ cm}^2$, and varies from 3 to 5 cm when lung SBRT treatments are applied (Pokhrel et al., 2020). Hence, even though the characterization of alanine dosimeter’s response to such small field was not the goal of this study, the results show the need of further studies for the use of alanine in smaller field sizes. The results show excellent agreement between ionization chamber and alanine for these configurations.

3.4. End to end test

Fig. 8 shows the axial sections of the phantom on the planning screen using VMAT technique with a prescribed dose of 18 Gy in the PTV.

After ESR spectrum recording, the dose in Alanine was determined using calibration curve (Fig. 6) and adjusted using Equation (2). Table 2 shows the results obtained in both phantoms and calculated by the treatment planning system. Table 3 the uncertainties associated to End-to-End test are reported.

It is observed that the doses calculated by the Planning System are similar to the alanine measurements for homogeneous regions. The nominal difference is 0.6% in relation to the average dose reported in TPS. The good agreement between planned and obtained dose with alanine dosimeters in applications similar to this work have been reported in the literature (Rech et al., 2014; Wagner 2008). Distefano et al., 2015 reports differences lesser than 0.4% between Alanine and

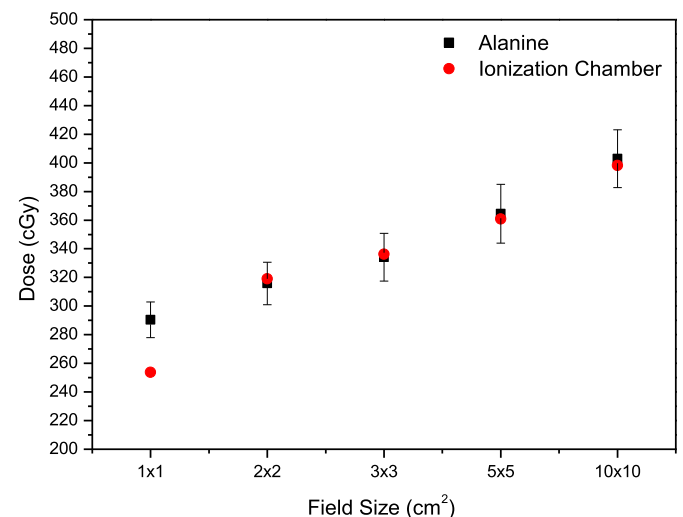


Fig. 7. Dose values according to field size. For the alanine dosimeter, each point (black) represents the average and standard deviation of dose obtained in 2 dosimeters and the ionization chamber (red) measurements is for 1 measurement. (For interpretation of the references to color in this figure legend, the reader is referred to the Web version of this article.)

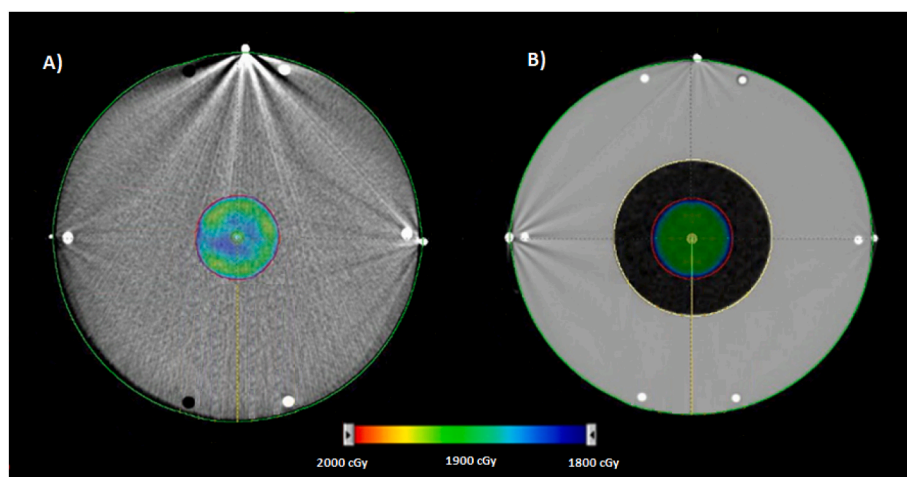


Fig. 8. Image of axial section of phantoms (a) homogeneous and (b) heterogeneous showing the SBRT planned doses with VMAT technique. Red line in central circle is the PTV, in which the dose map illustrates colored isodoses from 18 Gy (blue) to 20 Gy (red). (For interpretation of the references to color in this figure legend, the reader is referred to the Web version of this article.)

Table 2

Average and standard deviation of doses obtained in alanine and TPS in phantoms.

| Phantom | Dose Alanine (cGy) | Average TPS (cGy) |
|---------------|--------------------|-------------------|
| Homogeneous | 1834.0 ± 13.0 | 1844.5 ± 22.8 |
| Heterogeneous | 1952.9 ± 20.4 | 1867.6 ± 32.7 |

Table 3

Uncertainty associated to End-to-End test.

| Component | Uncertainty |
|-------------------------------------|-------------|
| Random Uncertainties | |
| Spectrometer stability | 0.50% |
| Analytical Balance | 0.50% |
| Irradiation | 0.50% |
| Dosimeters | 3.00% |
| Repeatability | 0.71% |
| Systematic Uncertainty | |
| ESR Calibration Curve | 0.50% |
| Results | |
| Coverage factor (k)* | 2.30 |
| Relative Combined Uncertainty | 2.00% |
| Uncertainty at 95% confidence level | 4.60% |

* t -Student's distribution.

TPS, film and farmer ionization chamber, in SBRT lung treatment performed in anthropomorphic thorax phantom. Also describe no significant difference between the performance of AAA and Monte Carlo algorithms. Reis et al. (2019) report high correlation of dose distribution in heterogeneous medium (water/lung/water) obtained using Monte Carlo simulation and dose calculation algorithms (AAA) and Acuros XB (TPS) for irradiation field of $2 \times 2 \text{ cm}^2$.

For the heterogeneous region and low density, as the lung, the difference between the average planned dose and the measured dose is 4.5%. As expected, larger differences were found for the heterogeneous phantom, showing the necessity of accurate dose assessment in such cases.

Therefore, with the End-to-End test, it was possible to verify all the steps of the treatment with very small discrepancy, from the acquisition of images to the delivery of the dose. The percent standard deviation of the doses assessed with the alanine dosimeters are 0.7% (13.0 cGy SD for

a dose of 1834.0 cGy) and 1.0% (20.4 cGy SD for a dose of 1952.9 cGy) in the case of homogeneous and heterogeneous phantom respectively, as can be seen in Table 2. The expanded uncertainty at 95% confidence level is 4.60%. Similar results of precision of dosimetry with alanine are reported by Carlino et al. (2018), in end-to-end tests for proton beam therapy. Thus, L-alanine detector is suitable for implementation in the SBRT quality control of small fields using VMAT. As a feasibility study, results of only one center were analyzed, however, it shows that a protocol for QA could be established with this dosimetric system. For instance, the phantom could be shipped to different hospitals for a treatment and after returning, the dose determined at the laboratory as an audit system.

4. Conclusions

L-alanine dosimeters bring together several advantageous aspects for use as a dosimetric system in SBRT QA using VMAT. It is tissue-equivalent, presents a linear correlation in the range of doses of interest, and high performance in irradiation fields sizes relevant for lung SBRT. The end-to-end test presented uncertainty at 95% confidence level of 4.60%.

Acknowledgements

We are grateful to CNPq Grants 304107/2019-0, 407471/2016-2, 309186/2020-0 and FAPESP Grants 2007/06720-4 and CEPID-NEUROMAT 13/07699-0, CAPES (finance code 0001), NAP-FisMed and INCA for partial financial and institutional support in several stages of this project. We are thankful to Lourenço Rocha, Carlos Brunello, Carlos Renato da Silva and Rafael de Barros for technical support.

References

- Abrego, F. C., Calcina, C. S. G., de Almeida, A., et al. (2007). Relative output factor and beam profile measurements of small radiation fields with an L-alanine/K-band EPR minidosimeter. *Med. Phys.*, 34(5), 1573–1582. <https://doi.org/10.1118/1.2717414>
- Alfonso, R., Andreo, P., Capote, R., Huq, M. S., Kilby, W., Kjäll, P., Mackie, T. R., Palmans, H., Rosser, K., Seuntjens, J., et al. (2008). A new formalism for reference dosimetry of small and nonstandard fields. *Medical Physics*, 35(11), 5179–5186. <https://doi.org/10.1118/1.3005481>
- Alves, G. G., Kinoshita, A., Oliveira, H. F. de, Guimarães, F. S., Amaral, L. L., & Baffa, O. (2015). Accuracy of dose planning for prostate radiotherapy in the presence of metallic implants evaluated by electron spin resonance dosimetry. *Brazilian Journal of Medical and Biological Research*, 48(7), 644–649.

- Anton, M., Kapsch, R. P., Krauss, A., von Voigts-Rhetz, P., Zink, K., McEwen, M., et al. (2013). Difference in the relative response of the alanine dosimeter to megavoltage x-ray and electron beams. *Physics in Medicine and Biology*, *58*, 3259–3282.
- Anton, M., Kapsch, R., Krystek, M., et al. (2008). Response of the alanine/ESR dosimetry system to MV x-rays relative to Co-60 radiation. *Phys. Med. Biol.* v., *53*(10), 2753–2770. <https://doi.org/10.1088/0031-9155/53/10/020>
- Baffa, O., & Kinoshita, A. (2014). Clinical applications of alanine/electron spin resonance dosimetry. *Radiation and Environmental Biophysics*, *53*(2), 233–3282. <https://doi.org/10.1007/s00411-013-0509-2>
- Carlino, A., Gouldstone, C., Kragl, G., et al. (2018). End-to-end tests using alanine dosimetry in scanned proton beams. *Phys. Med. Biol.* v., *63*(5), 55001. <https://doi.org/10.1088/1361-6560/aaac23>
- Chen, F., Nicolucci, P., & Baffa, O. (2008). Enhanced sensitivity of alanine dosimeters to low-energy X-rays: Preliminary results. *Rad. Meas.* v., *43*, 467–470. <https://doi.org/10.1016/j.radmeas.2007.11.066>
- Das, I. J., Ding, G. X., & Ahnesjö, A. (2007). Small fields: Nonequilibrium radiation dosimetry. *Medical Physics*, *35*(1), 206–215. <https://doi.org/10.1118/1.2815356>
- Distefano, G., Jafari, S. M., Lee, J., Gouldstone, C., Mayles, H. M. O., & Clark, C. H. (2015). UK SABR consortium lung dosimetry audit; absolute dosimetry results. In *Radiother oncol* (Vol. 115, pp. S75–S76). Barcelona: Elsevier Masson SAS. [https://doi.org/10.1016/S0167-8140\(15\)40153-7](https://doi.org/10.1016/S0167-8140(15)40153-7)
- Fuse, H., Fujisaki, T., Ikeda, R., et al. (2018). Alicability of lung equivalent phantom using the cork with absorbed water in radiotherapeutic dosimetry. *International Journal of Medical Physics, Clinical Engineering and Radiation Oncology*, *7*, 27–34. <https://doi.org/10.4236/ijmpcero.2018.71003>
- Helt-Hansen, J., Rosendal, F., Kofoed, I. M., & Andersen, C. E. (2009). Medical reference dosimetry using EPR measurements of alanine: Development of an improved method for clinical dose levels. *Acta Oncologica*, *48*(2), 216–222.
- ISO/IEC GUIDE 98-3 2008. (2008). Uncertainty of measurement — Part 3: Guide to the expression of uncertainty in measurement (GUM:1995). *Int Stand Organ Geneva*, *1*, 120. <https://www.iso.org/standard/50461.html>.
- Knudtsen, I. S., Svestad, J. G., Sande, E. P. S., Rekstad, B. L., Rødal, J., Van Elmpt, W., Öllers, M., Hole, E. O., & Malinen, E. (2016). Validation of dose painting of lung tumours using alanine/EPR dosimetry. *Physics in Medicine and Biology*, *61*(6), 2243.
- Kuntz, F., Pabst, J. Y., Delpech, J. P., Wagner, J. P., & Marchioni, E. (1996). Alanine-ESR in vivo dosimetry: A feasibility study and possible applications. *Applied Radiation and Isotopes*, *47*(11–12), 1183–1188.
- Li, Y., Ma, J., Chen, X., Tang, F., & Zhang, X. (2016). 4DCT and CBCT based PTV margin in Stereotactic Body Radiotherapy(SBRT) of non-small cell lung tumor adhered to chest wall or diaphragm. *Radiation Oncology*, *11*(1), 152.
- Merrow, C. E., Wang, I. Z., & Podgorsak, M. B. (2013). A dosimetric evaluation of VMAT for the treatment of non-small cell lung cancer. *Journal of Applied Clinical Medical Physics*, *14*(1), 228–238.
- Meyer, J. (2011). *IMRT, IGRT, SBRT: Advances in the treatment planning and delivery of radiotherapy* (2nd ed.). Basel: Karger Medical and Scientific Publishers.
- O'Daniel, J., Das, S., Wu, Q. J., & Yin, F.-F. (2012). Volumetric-Modulated Arc therapy: Effective and efficient end-to-end patient-specific quality assurance. *International Journal of Radiation Oncology, Biology, Physics*, *82*(5), 1567–1574.
- Onori, S., Bortolin, E., Calicchia, A., Carosi, A., De Angelis, C., & Grande, S. (2006). Use of commercial alanine and TL dosimeters for dosimetry intercomparisons among Italian radiotherapy centres. *Radiation Protection Dosimetry*, *120*(1–4), 226–229.
- Papanikolaou, N., Battista, J. J., Boyer, A. L., Kappas, C., Klein, E., Mackie, T. R., Sharpe, M., & Van Dyk, J. (2004). Tissue inhomogeneity corrections for megavoltage photon beams. *AAPM Task Gr*, *65*, 1–142.
- Parwaie, W., Refahi, S., Ardekani, M. A., & Farhood, B. (2018). Different dosimeters/detectors used in small-field dosimetry: Pros and cons. *J Med Signals Sens*, *8*(3), 195–203. https://doi.org/10.4103/jmss.JMSS_3_18
- Pokhrel, D., Halfman, M., & Sanford, L. (2020). FFF-VMAT for SBRT of lung lesions: Improves dose coverage at tumor-lung interface compared to flattened beams. *Journal of Applied Clinical Medical Physics*, *21*(1), 26–35.
- Ramírez, J. V., Marques, T., Chen, F., Nicolucci, P., & Baffa, O. (2012). Percentage depth dose curves comparison between L-alanine minidosimeters, radiographic film and PENELOPE Monte Carlo simulation for a 60Co beam. *Proceed. IRPA*, *12*, 91.
- Rech, A. B., Barbi, G. L., Ventura, L. H. A., Guimaraes, F. S., Oliveira, H. F., & Baffa, O. (2014). In vivo dose evaluation during gynaecological radiotherapy using L-alanine/ESR dosimetry. *Radiation Protection Dosimetry*, *159*(1–4), 194–198.
- Regulla, D. F., & Deffner, U. (1982). Dosimetry by ESR spectroscopy of alanine. *The International Journal of Applied Radiation and Isotopes*, *33*(11), 1101–1114.
- Reis, C. Q. M., Nicolucci, P., Fortes, S. S., & Silva, L. P. (2019). Effects of heterogeneities in dose distributions under nonreference conditions: Monte Carlo simulation vs dose calculation algorithms. *Medical Dosimetry*, *44*(1), 74–82.
- Rouihem, F., Hosni, F., Dridi, W., et al. (2022). Numerical analysis of the alanine response using Monte Carlo: Correlation with experimental results. *Radiation Physics and Chemistry*, *190*, 109824. <https://doi.org/10.1016/j.radphyschem.2021.109824>
- Rubio, C., Morera, R., Hernando, O., Leroy, T., & Lartigau, S. E. (2013). Extracranial stereotactic body radiotherapy. Review of main SBRT features and indications in primary tumors. *Reports of Practical Oncology and Radiotherapy*, *18*(6), 387–396.
- Secerov, B., Radenkovic, M., & Dramicanin, M. (2016). Uncertainty and routine use of Aerial L-alanine – electron spin resonance dosimetry system. *Rad. Meas.* v., *89*, 63–67. <https://doi.org/10.1016/j.radmeas.2016.03.003>
- Seravalli, E., Van Haaren, P. M. A., Van Der Toorn, P. P., & Hurkmans, C. W. (2015). A comprehensive evaluation of treatment accuracy, including end-to-end tests and clinical data, applied to intracranial stereotactic radiotherapy. *Radiotherapy & Oncology*, *116*(1), 131–138.
- Sharpe, P. H. G., Rajendran, K., & Sephton, J. P. (1996). Progress towards an alanine/ESR therapy level reference dosimetry service at NPL. *Applied Radiation and Isotopes*, *47* (11–12), 1171–1175.
- Simon, L., Giraud, P., Servois, V., et al. (2006). Initial evaluation of a four-dimensional computed tomography system, using a programmable motor. *J. Appl. Clin. Med. Phys.* v., *7*(4), 50–65. <https://doi.org/10.1120/jacmp.v7i4.2301>
- Sterpin, E., Tomsej, M., De Smedt, B., Reynaert, N., & Vynckier, S. (2007). Monte Carlo evaluation of the AAA treatment planning algorithm in a heterogeneous multilayer phantom and IMRT clinical treatments for an Elekta SL25 linear accelerator. *Medical Physics*, *34*(5), 1665–1677.
- Vanbree, N., Idzes, M., Huizenga, H., et al. (2014). Film dosimetry for radiotherapy treatment planning verification of a 6 MV tangential breast irradiation. *Radiat. Oncol.* v., *31*(3), 251–255. [https://doi.org/10.1016/0167-8140\(94\)90431-6](https://doi.org/10.1016/0167-8140(94)90431-6)
- Vega Ramirez, J. L., Chen, F., Nicolucci, P., & Baffa, O. (2011). Dosimetry of small radiation field in inhomogeneous medium using alanine/EPR minidosimeters and PENELOPE Monte Carlo simulation. *Radiation Measurements*, *46*(9), 941–944.
- Vega, R. J. L., Chen, F., Nicolucci, P., Apaza, V. D. G., Chen, F., & GCFO and, B. O. (2014). Tissue interfaces dosimetry in small field radiotherapy with alanine/EPR mini dosimeters and Monte Carlo-Penelope simulation. In *Int symp solid state dosim. Cusco, Peru* (pp. 1–9). Mexico: Sociedad Mexicana de Irradiación y Dosimetría.
- Wagner, D., Mathias, A., Vorwerk, H., et al. (2008). In vivo alanine/electron spin resonance (ESR) dosimetry in radiotherapy of prostate cancer: A feasibility study. *Radiotherapy & Oncology*, *88*, 140–147.